Journal of Molecular Structure 1259 (2022) 132736

Contents lists available at ScienceDirect

Journal of Molecular Structure

journal homepage: www.elsevier.com/locate/molstr

An investigation into the coordination chemistry of tripodal "click" triazole ligands with Mn, Ni, Co and Zn ions

Mariya Chernobryva[a], Majid Motevalli[a], Chris S. Hawes[b], Michael Watkinson[a,b,*]

[a] The Joseph Priestley Building, School of Biological and Chemical Sciences, Queen Mary University of London, Mile End Road, London, E1 4NS, UK
[b] School of Chemical and Physical Sciences, Keele University, Keele, ST5 5BG, UK

ARTICLE INFO

Article history:
Received 27 October 2021
Revised 25 January 2022
Accepted 27 February 2022
Available online 2 March 2022

Keywords:
Tripodal ligands
Click triazoles
Intermolecular interactions
d-block coordination compounds

ABSTRACT

The steric influences of the triazole side chains in two tripodal chelating ligands tris[(1-*benzyl*-1H-1,2,3-*triazol*-4-*yl*)*methyl*]amine (TBTA) and tris[(1-*phenyl*-1H-1,2,3-*triazol*-4-*yl*)*methyl*]amine (TPTA) are explored through structural studies of four new mononuclear *d*-block metal complexes. The manganese(II) complex $[Mn(TPTA)_2](ClO_4)_2{\cdot}H_2O$ **1** includes two TPTA ligands each coordinated in a tridentate fashion to give an unusual trigonal prismatic coordination geometry with two non-coordinated pendant triazole groups which engage in weak hydrogen bonding interactions. $[Ni(TBTA)(OH_2)Cl]Cl{\cdot}3H_2O{\cdot}MeCN$ **2** contains an octahedral nickel(II) centre bound by a tetradentate TBTA ligand along with aqua and chloride ligands, where the significant degree of lattice solvation leads to an extensive hydrogen bonding network linking complexes through hexa-aqua water clusters. The mononuclear copper(II) complex $[Cu(TPTA)Cl_2]{\cdot}MeCN$ **3** contains no classical hydrogen bond donors but instead intermolecular aggregation takes place through chelating C–H···Cl hydrogen bonds involving the acidic triazole C–H groups which leads to close association of adjacent complexes. The zinc complex $[Zn(TPTA)Cl]_2[ZnCl_4]{\cdot}MeOH$ **4**, in which cationic $[Zn(TPTA)Cl]^+$ species are accompanied by tetrachlorozincate anions, exhibits a tris-triazole chelating coordination geometry for the TPTA ligand and associates through tetrameric $\pi\cdots\pi$ stacking interactions despite the positive charge present on each species. Structural analysis of these complexes, supported by solution-state mass spectrometry, NMR spectroscopic and magnetic susceptibility measurements, where applicable, provides new insights into the breadth of coordination geometries and intermolecular packing modes available to this important class of chelating ligand.

1. Introduction

Tripodal chelating ligands have a rich and diverse coordination chemistry. Historically, tripodal nitrogen-donor ligands have been key species in understanding stereochemistry in coordination compounds [1], and key catalytic species for various organic transformations [2]. Despite their long history, they continue to find contemporary applications in a number of areas including, but not limited to, organometallic chemistry [3], molecular magnetism [4], photochemistry [5], and catalysis [6]. The use of 'click' triazole-based ligands in particular has received recent attention because straightforward synthesis and derivatization can give modular families of ligands for structure-function studies [7], which is particularly useful in tuning molecular magnetism properties. For example, Schweinfurth *et al.* demonstrated that coordinating cobalt(II) with TBTA resulted in spin crossover behaviour at elevated temperatures [8]. Within this broad ligand class the ligands tris[(1-*benzyl*-1H-1,2,3-*triazol*-4-*yl*)*methyl*]amine (TBTA) and tris[(1-*phenyl*-1H-1,2,3-*triazol*-4-*yl*)*methyl*]amine (TPTA), shown in Fig. 1, are examples of the emerging triazole-based ligands that can be prepared by the popular copper(I) catalysed 'click' cycloaddition between azides and alkynes [9]. Indeed TBTA has long been known to enhance the rate of the copper(I) catalysed 'click' cycloaddition [10]. The coordination chemistry of these ligands has been compared to the related pyridine-based tripodal ligands, such as tris(2-picolyl)amine (TPMA). For example, examining a series of further reports from Schweinfurth *et al.* [11] allows comparison between two tripodal cobalt(II) complexes of ligands TBTA and TPMA. The Co-N(triazole) bond distances in the [Co(TBTA)Cl]Cl complex are 0.03–0.05 Å shorter compared to the equivalent Co-N(pyridine) distances in [Co(TPMA)Cl]Cl. However, the distances between the metal and central tertiary amine nitrogen in [Co(TBTA)Cl]Cl and [Co(TPMA)Cl]Cl are 2.350(3) Å and 2.184(6) Å respectively, indicating that Co-N bond in the TBTA complex is acting as a capping

* Corresponding author at: School of Chemical and Physical Sciences, Keele University, Keele, ST5 5BG, UK.
E-mail address: m.watkinson@keele.ac.uk (M. Watkinson).

https://doi.org/10.1016/j.molstruc.2022.132736

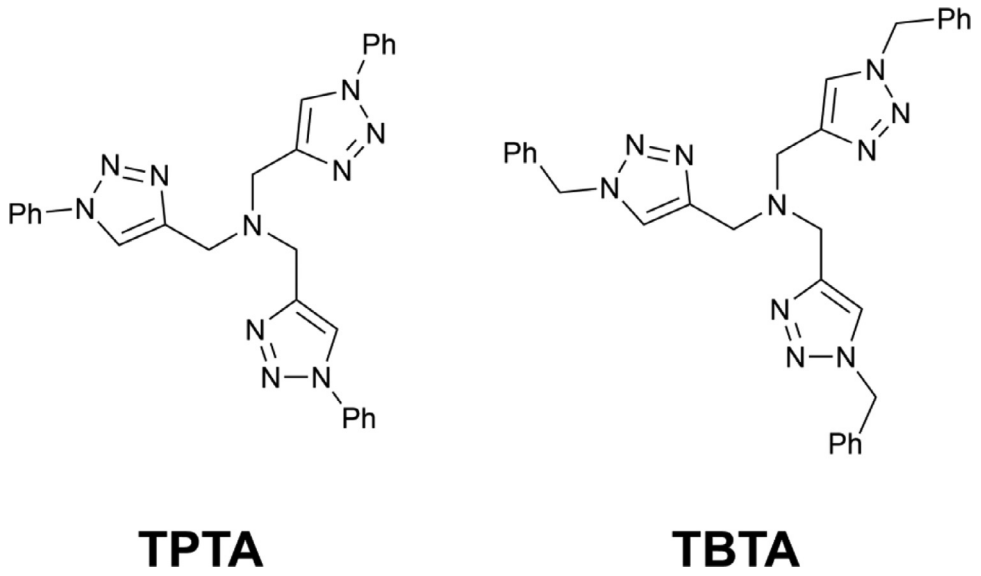

Fig. 1. The structure of ligands TPTA and TBTA.

bond with the coordination geometry described as capped tetrahedral or pseudo-tetrahedral 4 + 1, whereas the TPMA complex adopts a more regular trigonal bipyramidal geometry.

A salient example of the additional structural flexibility in tripodal triazole chelates was presented by Donnelly *et al.* [12]. This work reported an unusual dinuclear copper(I) complex of TBTA in which each metal cation adopts a distorted tetrahedral geometry with one triazole unit from each TBTA ligand bridging between two metal centres. In other cases, such as $[Ni(TBTA)_2](BF_4)_2$, the TBTA ligand was shown to act as a tridentate ligand, rather than a tetradentate ligand, further demonstrating the rather more unpredictable nature of the coordination chemistry of such ligands compared to homoleptic chelating ligands. The effect of structural modifications in the triazole-based ligands on the properties of their corresponding metal complexes has not yet received much attention [8,11,13,14].

In this report we survey a number of metal complexes of TBTA and its structural derivative TPTA, focusing on single crystal X-ray crystallography supported by solution-state spectroscopic methods. These methods were also used to examine to what extent this small structural variation in the 'click'-derived triazole ligand can tune the structural and electronic properties of their corresponding metal complexes.

2. Experimental

2.1. Materials and methods

All commercially available precursors and reagents were obtained from Sigma Aldrich and CheMatech and used as received. The ligands TPTA and TBTA were prepared according to previously reported methods (ESI) [15]. Infrared spectra were recorded in the range 4000–600 cm^{-1}, obtained directly from the compound as a solid on a Bruker Tensor 37 FTIR spectrometer. ^1H NMR and ^{13}C NMR spectra were recorded on either Bruker AV400 or AVIII400 NMR spectrometers (^1H NMR: 400 MHz; ^{13}C NMR: 100 MHz). The deuterated solvents used to record the spectra are stated before each set of data. Chemical shifts are reported in ppm and referenced to residual protonated solvent. Multiplicity is given as follows: *s* = singlet *m* = multiplet, and coupling constants are reported to 1 dp. Effective magnetic moments (μ_{eff}) were determined by the Evans' NMR spectroscopy method [16] in CD_3CN/MeCN/TMS solution at room temperature on a Bruker AVIII400 NMR spectrometer. UV–Vis spectra were obtained on an HP 8453 and Varian Cary 300 Bio UV-Visible spectrophotometers and absorption maxima (λ_{max}) together with the molar extinction coefficients (ε) are reported. High resolution electrospray ionisation mass spectrometry was carried out by the EPSRC National Mass Spectrometry Service, University of Wales, Swansea on a Thermofisher LTQ Orbitrap XL. Melting points were measured on a Stuart SMP3 melting point apparatus and are uncorrected.

2.2. X-ray crystallography

The data were collected on a Bruker Kappa Apex Duo diffractometer with an Apex-II area detector and a molybdenum sealed tube X-ray source (λ = 0.71073 Å). The crystal-to-detector distance was 30 mm and the data were measured using ϕ and Ω scans (2.0° increments, 10 s exposure time). Data collection and processing were carried out using the Bruker APEXII software package [17] and multi-scan absorption corrections was applied using SADABS [18]. The structures were solved using direct-methods with the program SHELXS-2014/7 [19] and refined anisotropically (non-hydrogen atoms) by full-matrix least-squares on F^2 using SHELXL-2014/7 [20], with further processing and analysis performed using the Olex2 software package [21]. The H atom positions were calculated geometrically and refined with a riding model with O–H distance restraints applied where appropriate. Crystal and refinement parameters are presented in Table S1 (ESI). CCDC 2101711-2101714.

2.3. Synthesis of $[Mn(TPTA)_2](ClO_4)_2{\cdot}H_2O$ 1

The ligand TPTA (100 mg, 0.204 mmol) and $Mn(ClO_4)_2{\cdot}6H_2O$ (36.9 mg, 0.102 mmol) were combined in MeOH (10 mL) and stirred at room temperature for 16 h. Following this period, any insoluble material was removed by filtration and diethyl ether (30 mL) was added, precipitating complex 1 as a beige solid (84 mg, 80%). Slow diffusion of Et_2O into a MeOH solution of this solid gave colourless single crystals of the title compound. μ_{eff}= 5.3 μ_B; ν_{max} (ATR, cm^{-1}) 3426, 3150, 1634, 1597, 1400, 1356, 1245, 1068, 992, 875; HRMS (EI) calcd for $C_{54}H_{49}N_{20}$ $[M + H]^+$ 977.4444, found: 977.4427 (HL^+ only, no complex detected).

2.4. Synthesis of [Ni(TBTA)(OH_2)Cl]Cl·3H_2O·MeCN 2

The ligand TBTA (100 mg, 0.188 mmol) and $NiCl_2·6H_2O$ (44.7 mg, 0.188 mmol) were combined in MeCN (10 mL) and stirred at room temperature for 16 h. Following this period the solution was filtered and diethyl ether (30 mL) was added to the filtrate to yield complex 2 as a crystalline green solid (101.5 mg, 82%). Slow diffusion of Et_2O into a MeCN solution of this solid resulted in single crystals of [Ni(TBTA)(OH_2)Cl]Cl·3H_2O·MeCN. m.p. 187–190 °C; μ_{eff}= 2.8 μ_B; IR: ν_{max} (ATR, cm^{-1}) 3058, 1618, 1492, 1455, 1331, 1248, 1135, 1074, 960, 804; UV–Vis (MeCN) λ_{max} /nm (ε/ $dm^3mol^{-1}cm^{-1}$) 367 (69), 580 (17), 790 (7), ~900 (11); HRMS (EI) calcd for $C_{30}H_{30}N_{10}NiCl$ $[M]^+$ 623.1697, found: 623.1689.

2.5. Synthesis of [Cu(TPTA)Cl_2]·MeCN 3

The ligand TPTA (100 mg, 0.204 mmol) and $CuCl_2·2H_2O$ (34.8 mg, 0.204 mmol) were combined in MeOH (10 mL) and stirred for 16 h at room temperature. The solution was filtered and diethyl ether (30 mL) was added, to yield complex 3 as a green solid (110 mg, 86%). Single crystals of [Cu(TPTA)Cl_2]·MeCN were grown from CD_3CN/MeCN. m.p. 160–162 °C; μ_{eff}= 1.7 μ_B; ν_{max} (ATR, cm^{-1}) 3434, 3068, 1595, 1499, 1456, 1348, 1254, 1192, 1082, 1046, 911, 831; UV–Vis (MeCN): λ_{max} /nm (ε/ $dm^3mol^{-1}cm^{-1}$) 360 (922), 650–700 nm- very broad (140); HRMS (EI) calcd for $C_{27}H_{24}N_{10}CuCl$ [M-Cl]$^+$ 586.1170, found: 586.1160.

2.6. Synthesis of [Zn(TPTA)Cl]$_2$[$ZnCl_4$]·MeOH 4

The ligand TPTA (100 mg, 0.204 mmol) and $ZnCl_2$ (55.6 mg, 0.408 mmol) were combined in MeOH (10 mL) and stirred at room temperature for 16 h. After filtration, diethyl ether (30 mL) was added to yield complex 4 as a beige solid (100 mg, 86%). Single crystals of [Zn(TPTA)Cl]$_2$[$ZnCl_4$]·MeOH were isolated from a solution of 4 in CD_3OD. m.p. 176–178 °C; ^{1}H NMR (400 MHz, DMSO–d_6): δ= 3.91 (s, 6H, N–CH_2), 7.47–7.50 (m, 3H, Ar-H), 7.58–7.62 (m, 6H, Ar-H), 7.90–7.92 (m, 6H, Ar-H), 8.76 (s, 3H, $CH_{triazole}$); ^{13}C NMR (DEPT 135, 100 MHz, DMSO–d_6): δ= 47.7, 120.0, 122.2, 128.5, 129.8, 136.6, 144.9; ν_{max} (ATR, cm^{-1}) 3480, 3075, 1596, 1499, 1466, 1354, 1249, 1193, 1085, 1045, 991, 965, 827 cm^{-1}; HRMS (EI) calcd for $C_{27}H_{24}N_{10}ZnCl$ $[M]^+$ 587.1160, found: 587.1150.

3. Results and discussion

The two ligands TPTA and TBTA were prepared according to previously published methods, [15] and all characterisation data were consistent with that previously reported. To generate crystalline metal complexes for analysis, each ligand was combined with the appropriate metal salt in either methanol or acetonitrile with stirring at room temperature which, after addition of diethyl ether, precipitated each of the four complexes 1 – 4. Diffusion of diethyl ether vapour or crystallisation from NMR samples were used to generate crystals suitable for analysis by single crystal X-ray diffraction. The structural information obtained from the diffraction experiments was supported by solution-state characterisation methods (EI-MS, UV-Visible and NMR spectroscopy and magnetic susceptibility measurements using the Evans' method) and solid-state characterisation (FTIR).

3.1. Structure of [Mn(TPTA)$_2$](ClO_4)$_2$·H_2O 1

The diffraction data for complex 1 were solved and refined in the monoclinic space group $P2_1/c$. The asymmetric unit contains one manganese(II) cation coordinated by two tridentate TPTA ligands with two non-coordinating perchlorate anions providing charge balance, and a lattice water molecule. The coordination geometry of the manganese ion, shown in Fig. 2, is highly distorted tending towards trigonal prismatic geometry and exhibits substantial variations in Mn-N bond lengths. Each ligand coordinates through the amine nitrogen atom and two of the three triazoles. Both amine nitrogen atoms exhibit longer Mn-N distances than the triazole nitrogen atoms (2.478(2) and 2.531(2) Å for N5 and N1, respectively, *cf.* 2.16 – 2.23 Å for the triazoles). Combined, the strained geometry and relatively long Mn-N bond lengths in 1 indicate comparatively weak binding, and indeed complex 1 was the only compound studied which could not be detected by electrospray mass spectrometry, suggesting that this species does not persist under these ionization conditions. The magnetic moment of 1 was measured in solution at 5.3 μ_B, close to the spin-only value of 5.9 μ_B for the high-spin d^5 configuration.

The two non-coordinating triazole rings contain unbound Lewis acid and base character, and engage in distinct non-covalent interactions. While N13 adopts a relatively close approach to a vacant face of the manganese ion (distance N13···Mn1 3.151(2) Å) the directionality of this interaction is not consistent with a capping coordination bond. Instead, the N13-N15 ring accepts weak hydrogen bonds from the triazole C–H and methylene CH_2 group of an adjacent arm, at C···N distances of 3.175(3) and 3.529(3) Å but with relatively small C–H···N angles of 135° and 158°, respectively (Fig. 2B). The acidic C–H group of this triazole C12 donates a hydrogen bond to the lattice water molecule (C···O distance 3.034(3) Å, C–H···O angle 143°).

The remaining non-coordinating triazole N16-N18 exhibits different hydrogen bond acceptor character, accepting a hydrogen bond from the lattice water molecule at N16 (O···N distance 2.995(3) Å, O–H···N angle 159°) and a weaker C–H···N contact from a nearby phenyl C–H group at N17 (C···N distance 3.404(3) Å, C–H···N angle 146° All of the coordinating triazoles engage in C–H···O hydrogen bonding with the perchlorate anions. The C···O distances for these interactions fall in the range 3.184(3) – 3.362(3) Å. These contacts are uniformly longer than those for the non-coordinating triazoles, with the added benefit of an anionic acceptor, implying that metal coordination does not significantly increase the C–H donor ability in this instance.

The other predominant non-covalent contacts within the extended structure of 1 are π-π stacking interactions involving the conjugated phenyltriazole arms. Both face-to-face and edge-to-face contacts help to define a densely packed extended structure. The most significant such interactions are two centrosymmetric tetrads in which intramolecular head-to-head stacks between coordinating and non-coordinating aryltriazoles are further linked through a head-to-tail contact with an adjacent complex, as shown in Fig. 3. Interestingly, while this interaction is repeated for both non-equivalent ligands, the geometry of the stacks differs by the dihedral angle of the terminal head-to-head pairing.

3.2. Structure of [Ni(TBTA)(OH_2)Cl]Cl·3H_2O·MeCN 2

The diffraction data for complex 2 were solved and refined in the monoclinic space group $P2_1/c$. The asymmetric unit contains one nickel(II) cation coordinated by a single tetradentate TBTA ligand coordinated through the amine and all three triazole arms, as shown in Fig. 4. The remaining coordination sites, in a *cis* configuration, are occupied by a chlorido ligand (orientated *trans* to the amine), and an aqua ligand. While the amine nitrogen atom exhibits a longer Ni-N distance of 2.213(2) Å compared to the triazoles (2.060(2) – 2.116(2) Å), the octahedral geometry of the coordination sphere is comparatively regular with all *cis* angles falling in the range 77.50(6) – 97.97(5)°. A further non-coordinating chloride ion is present within the asymmetric unit, alongside three lattice water molecules and one acetonitrile molecule.

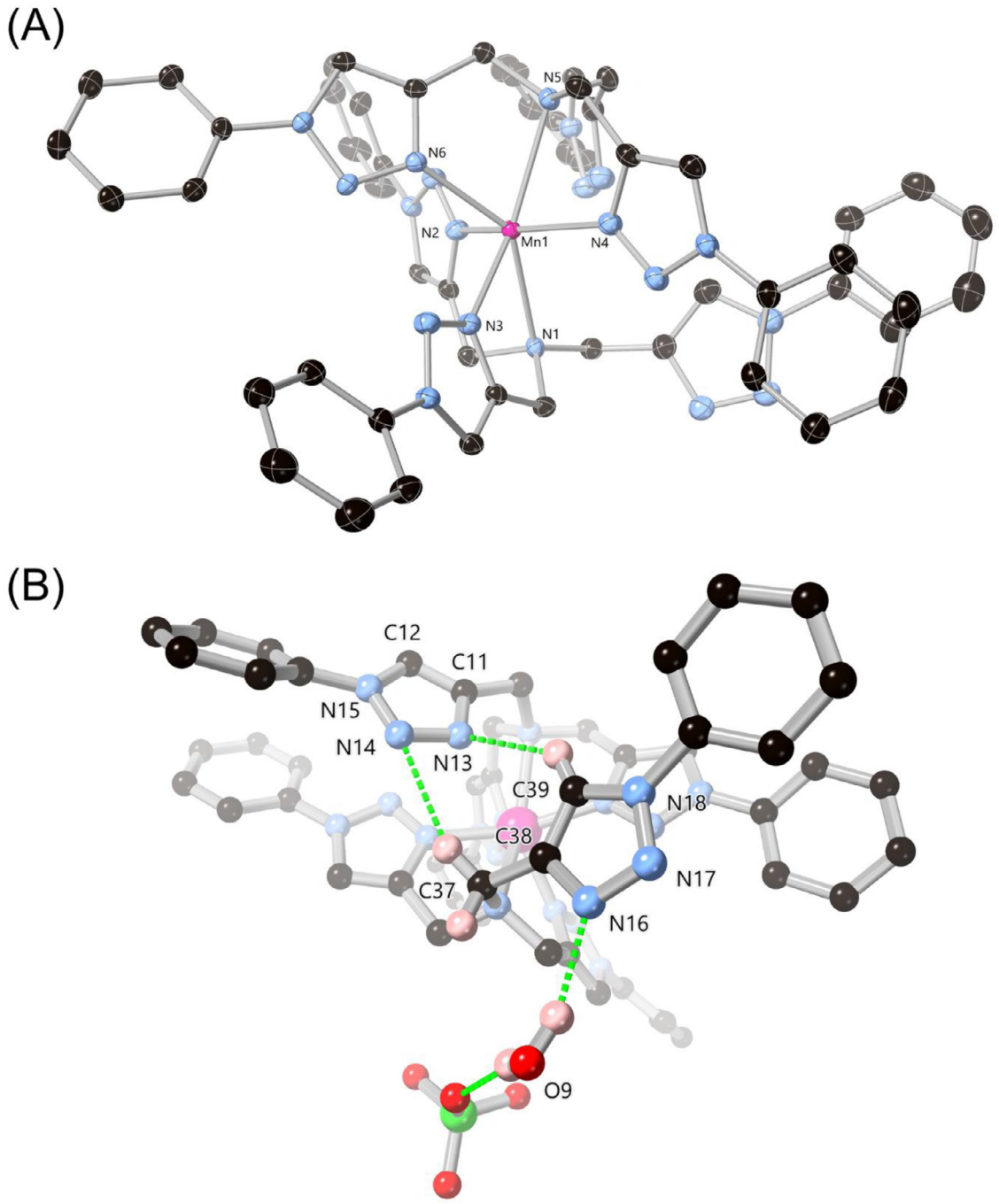

Fig. 2. (A) Structure of the $[Mn(TPTA)]^{2+}$ dication in the structure of 1 with labelling scheme for selected atoms. Hydrogen atoms, anions and solvent molecules are omitted for clarity. ADPs are rendered at 50% probability level. (B) The C–H···N contacts and other interactions involving the non-coordinating triazole arms in the structure of 1 with relevant atoms labelled.

The predominant intermolecular interactions in the structure of 2 are hydrogen bonds involving the aqua and chlorido ligands of the complex and the lattice chloride anion and water molecules, as shown in Fig. 5. The complex itself donates two hydrogen bonds through the aqua ligand and receives one hydrogen bond from lattice water O4 to the chlorido ligand. The lattice water molecules are arranged in centrosymmetric chair-shaped hexamers. Two faces of these clusters are capped by the nickel complexes, while the clusters are linked into a two-dimensional network by bridging through the lattice chloride anion, which accepts three hydrogen bonds (two from lattice water molecules and one from the aqua ligand). No significant C–H hydrogen bonding is observed from the triazole C–H groups in complex 2, and the remaining inter-complex interactions are relatively diffuse. This is most likely a consequence of the more substantial hydrogen bonding interactions from the water molecules dictating the extended structure.

Unlike complex 1, complex 2 was readily detected by electrospray mass spectrometry as the singly charged $[NiCl(TBTA)]^{+}$ cation following loss of the coordinated water molecule. The magnetic moment of 2.8 μ_B is as expected (calc. 2.83 μ_B) for a magnetically dilute d^8 Ni^{2+} complex. Electronic absorbances are observed at 367, 580, 790 and *ca.* 900 nm which are similar to those reported for polypyridyl ligand complexes of Ni(II) and is character-

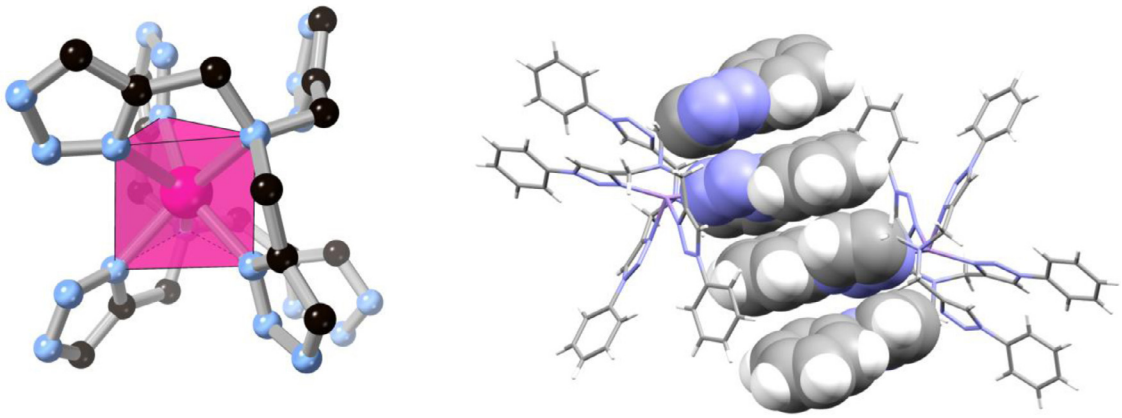

Fig. 3. (Left) Polyhedral representation of the trigonal prismatic coordination geometry of the manganese ion in complex 1. The ligand molecule is truncated for clarity. (Right) The discrete tetrameric π-π stacking interaction between two adjacent cations of complex 1.

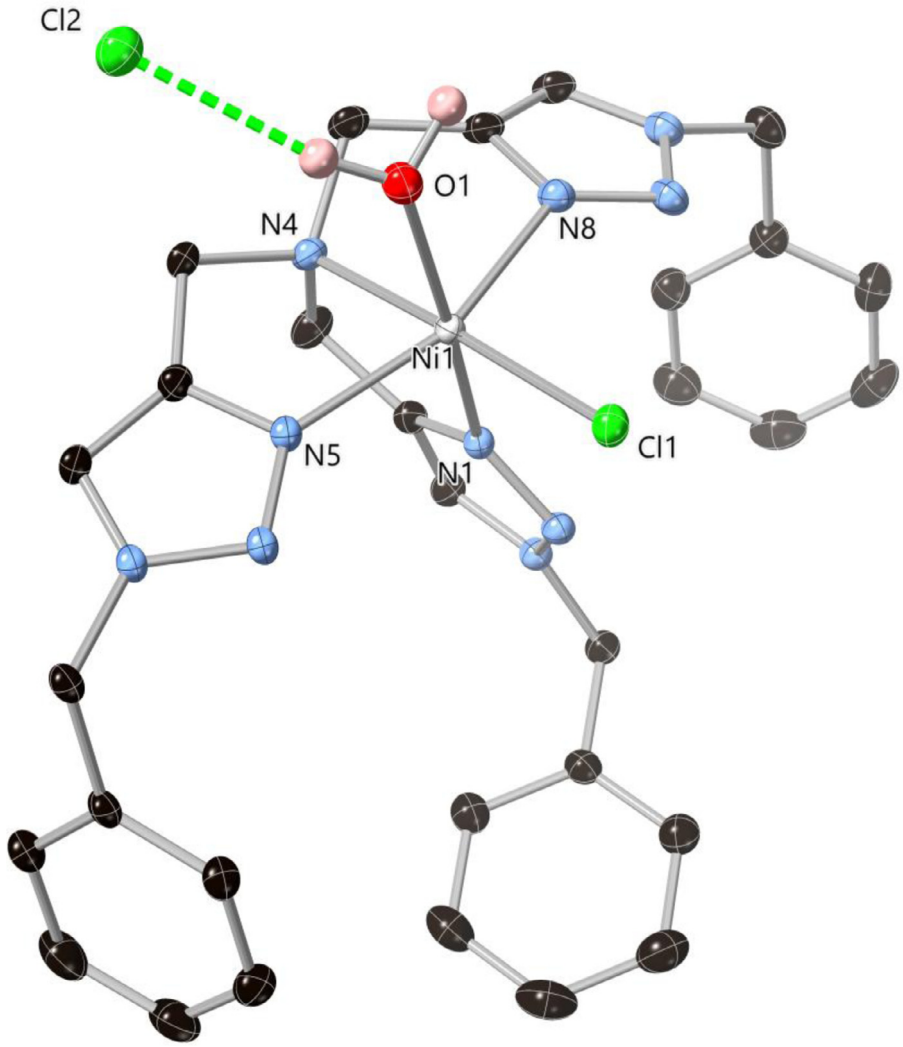

Fig. 4. The structure of complex 2 with partial atom labelling scheme. Hydrogen atoms and lattice water molecules are omitted for clarity, and ADPs are rendered at 50% probability level.

istic of d^8 Ni(II) in a pseudo-octahedral coordination. According to Hadadzadeh *et al.* [22], there are three spin-allowed transitions known for such octahedral Ni(II) complexes from the $^3A_{2g}$ ground state to the three triplet excited states: $^3A_{2g}(^3F) \rightarrow {}^3T_{2g}$, $^3A_{2g}(^3F) \rightarrow {}^3T_{1g}(^3F)$ and $^3A_{2g}(^3F) \rightarrow {}^3T_{1g}(^3P)$, with ε in the range of 18 to 27 $dm^3mol^{-1}cm^{-1}$. Thus, the three lowest energy absorption bands observed in the spectra reported here are most likely to correspond to these transitions while we ascribe the stronger, higher energy absorbance at 367 nm to either an MLCT or π-π^* transition involving the TBTA ligand.

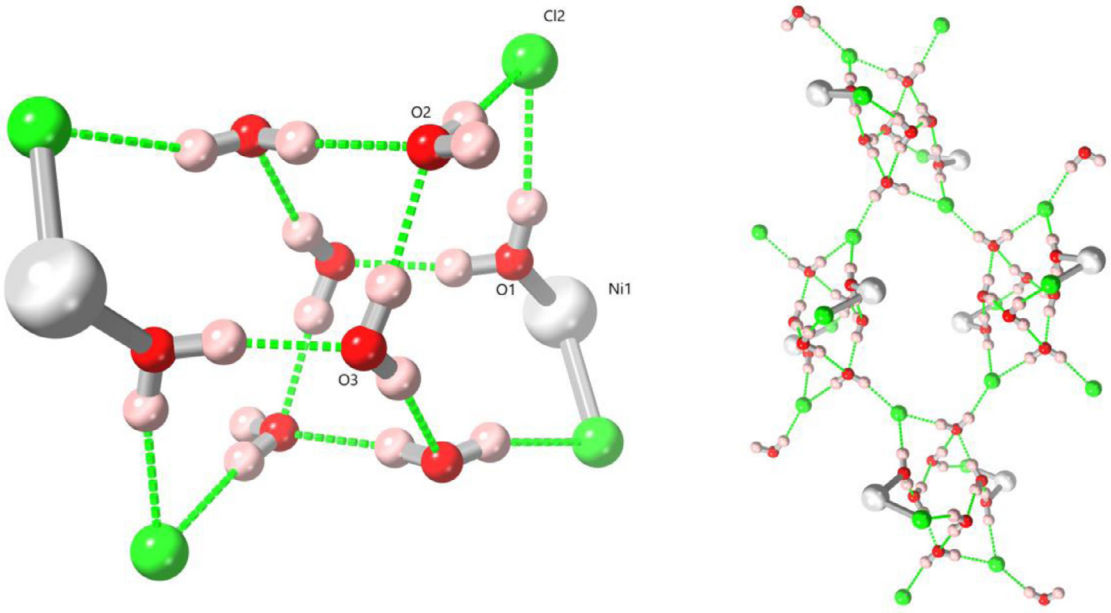

Fig. 5. (Left) Structure of an individual water cluster in 2, capped by two complexes of 2 and two lattice chloride anions. Labelling scheme is shown for unique heteroatoms. (Right) Linkage of discrete water clusters into the extended 2-dimensional network in the structure of 2 through the diverging hydrogen bonds donated from water molecule O2.

3.3. Structure of $[Cu(TPTA)Cl_2]\cdot MeCN$ 3

The diffraction data for complex 3 were solved and refined in the monoclinic space group $P2_1/n$. The asymmetric unit of 3 contains one copper(II) ion coordinated by one molecule of TPTA and two chlorido ligands, as shown in Fig. 6. One non-coordinating acetonitrile molecule is also present within the asymmetric unit. The TPTA ligand coordinates in a meridional tridentate fashion through the amine and two of the three triazoles, with the amine orientated *trans* to one chlorido ligand in the basal plane and the apical position occupied by the other chlorido ligand. The apical chlorido ligand Cl2 unsurprisingly shows a longer Cu-Cl bond distance of 2.4430(4) Å compared to Cl1 (2.2177(3) Å). This is consistent with the low τ_5 value of 0.05 indicating a stronger tendency towards square pyramidal geometry compared to trigonal bipyramidal [23]. Unlike in complex 1, the non-coordinating phenyltriazole arm is orientated outwards from the metal binding site and does not undergo any substantial intramolecular contacts with the rest of the molecule.

Lacking any classical hydrogen bond donors, the most substantial intermolecular contacts in the extended structure of 3 are weaker C–H···Cl contacts. These are readily visualised on a normalised contact distance mapping of the Hirshfeld surface [24], and the most notable features from the corresponding fingerprint plot (Fig. 7) which reveals multiple short contacts involving the apical chlorido ligand Cl2 as the acceptor. A chelate-type interaction to this acceptor is observed from the non-coordinating triazole C–H and *ortho* C–H group of the attached phenyl from an adjacent complex. The C···Cl distances of 3.7238(11) and 3.6897(12) Å for C20 and C26, and C–H···Cl angles of 167° and 169°, respectively, indicate roughly equivalent contribution from both donors. Further contacts to this chlorido ligand are observed from the lattice acetonitrile molecule, and a further C–H contact from a coordinated triazole C12 which is bifurcated between the two chlorido ligands. Additional π-π interactions are observed throughout the extended structure, including a centrosymmetric head-to-tail interaction between the non-coordinating phenyltriazole arm at a mean interplanar distance of 3.42 Å. The axial bulk of the complex interrupts any large scale π-π overlap across the basal plane of the complex with only minor aryl-aryl contacts at the periphery for the coordinating arms.

The effective magnetic moment for complex 3 of 1.7 μ_B was consistent with expectations for a d^9 Cu^{2+} species (calc. 1.7 μ_B), and electrospray mass spectrometry results showed the persistence of the complex in solution with detection of the $[CuCl(TPTA)]^+$ cation. Electronic spectroscopy revealed a typical MLCT transition centred at 360 nm as well as a broad absorbence in the range 650 – 700 nm, which is similar to that reported for the tetradentate Cu(II) complex $[Cu(TMPA)Cl]PF_6$ which adopts trigonal bipyramidal geometry [25].

3.4. Structure of $[Zn(TPTA)Cl]_2[ZnCl_4]\cdot MeOH$ 4

The diffraction data for compound 4 were solved and refined in the chiral monoclinic space group $P2_1$. The asymmetric unit contains two [Zn(TPTA)Cl] cations, a tetrachlorozincate dianion and a lattice methanol molecule, as shown in Fig. 8. The two cations are almost geometrically identical; both contain a four-coordinate zinc adopting a tetrahedral geometry bound by three triazole nitrogen atoms and a chlorido ligand. All Zn-N bonds from the triazole nitrogen atoms fall in the range 2.022(3) – 2.057(3) Å. Although the lone pair from the central amine of TPTA is orientated towards the metal ion, the N-Zn distance (2.585(3) and 2.5999(3) Å for Zn1 and Zn2, respectively) is too long to be considered a formal coordination bond. Indeed, the zinc ions themselves show little deviation from the ideal tetrahedral geometry with no notable tendency towards trigonal pyramidal geometry; both zinc ions reside 0.66 Å from the mean plane of the three coordinating triazole nitrogen atoms. The tetrachlorozincate anion also exhibits a regular tetrahedral geometry with all Cl-Zn-Cl angles falling in the range 106.85(4) – 114.34(4).

The complexes themselves take on a threefold propeller geometry at the triazoles, although the phenyl rings show varying degrees of distortion from coplanarity with the attached triazoles, with dihedral angles 10.6(5), 33.3(5) and 77.1(5)° for the Zn2 residue and essentially equivalent values for the Zn1 case. Intermolecular interactions in the structure of 1 involve C–H···Cl hydrogen bonds from the triazole C–H groups to the chlorido ligands

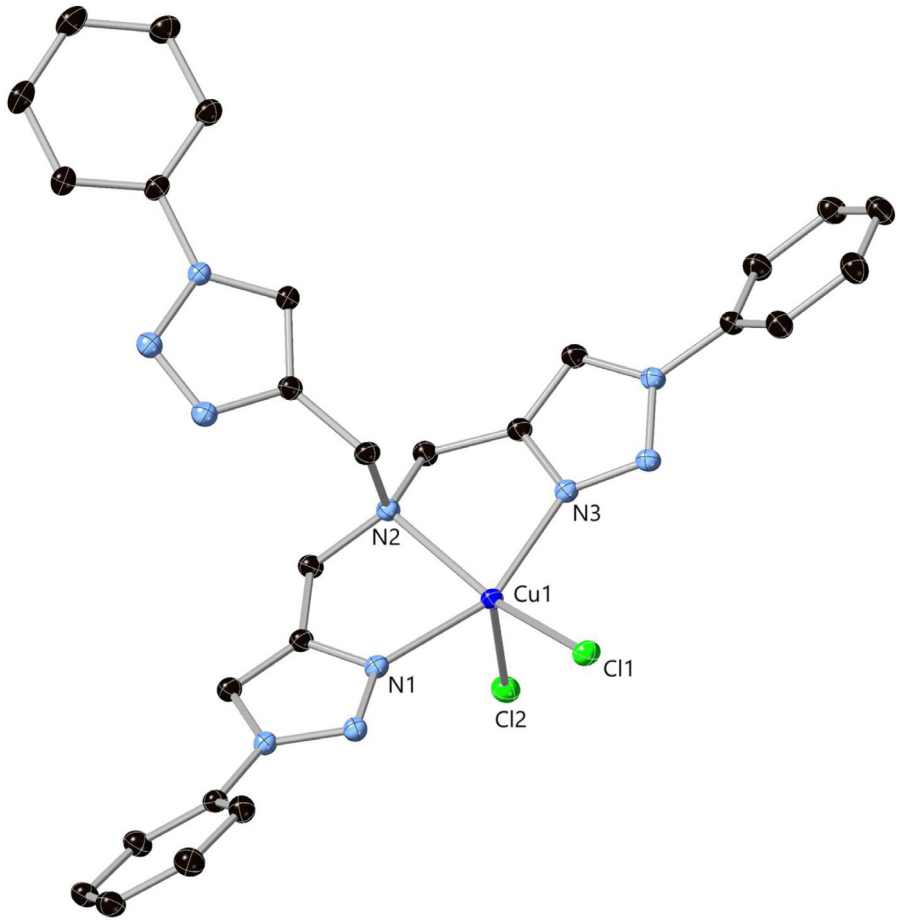

Fig. 6. Structure of complex 3 with labelling scheme for selected heteroatoms. Hydrogen atoms are omitted for clarity and ADPs are rendered at the 50% probability level.

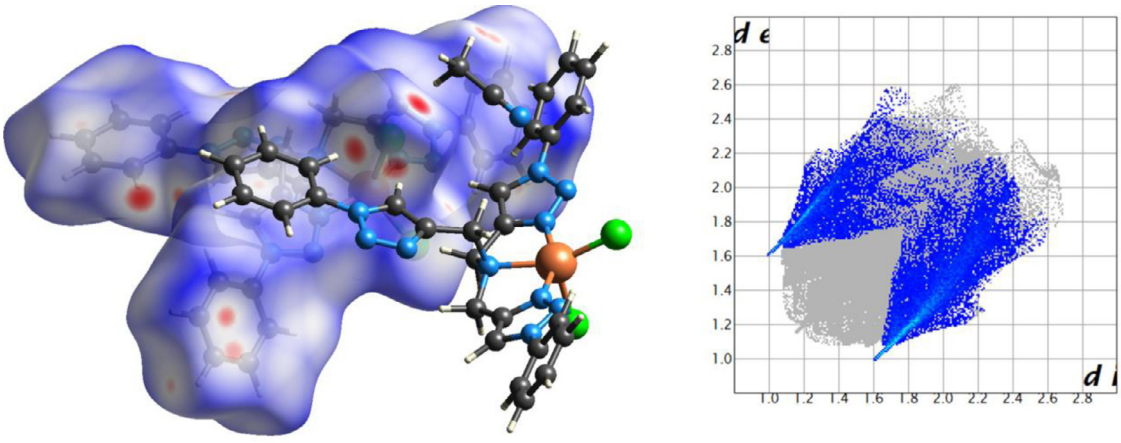

Fig. 7. (Left) The weak C–H···Cl contacts in the structure of 3 represented on a normalised contact map of the Hirshfeld surface, where close contacts are represented in red (surface isovalues −0.15/+1.15). (Right) Fingerprint plot for compound 3 with H···Cl contacts highlighted showing the directional nature of these contacts.

of either the tetrachlorozincate or an adjacent [Zn(TPTA)Cl] cation, and these features are again clearly visible on the normalized contact distance mapping of the Hirshfeld surface and the associated fingerprint plot (ESI, Figs. S2-S3). The lattice methanol molecule also donates a strong hydrogen bond to a chlorido ligand of the tetrachlorozincate anion at an O···Cl distance of 3.132(5) Å. The other noteworthy non-covalent interaction in the structure of 4 is a π-π stacked tetrad linking four distinct cations, shown in Fig. 9. Though somewhat reminiscent of the interaction seen in 1 (though fully intermolecular), this contact involves only the triazole rings of the outer-most groups and the phenyl ring of the innermost, with these inner rings exhibiting the largest phenyl-triazole dihedral angle.

Electrospray ionization mass spectrometry showed unambiguously the persistence of the $[ZnCl(TPTA)]^+$ cation in solution. Although the diamagnetic nature of Zn^{2+} allowed straightforward collection of NMR data on the complex in d_6-DMSO, the chemical shifts observed (for both ^1H and ^{13}C nuclei) were essentially iden-

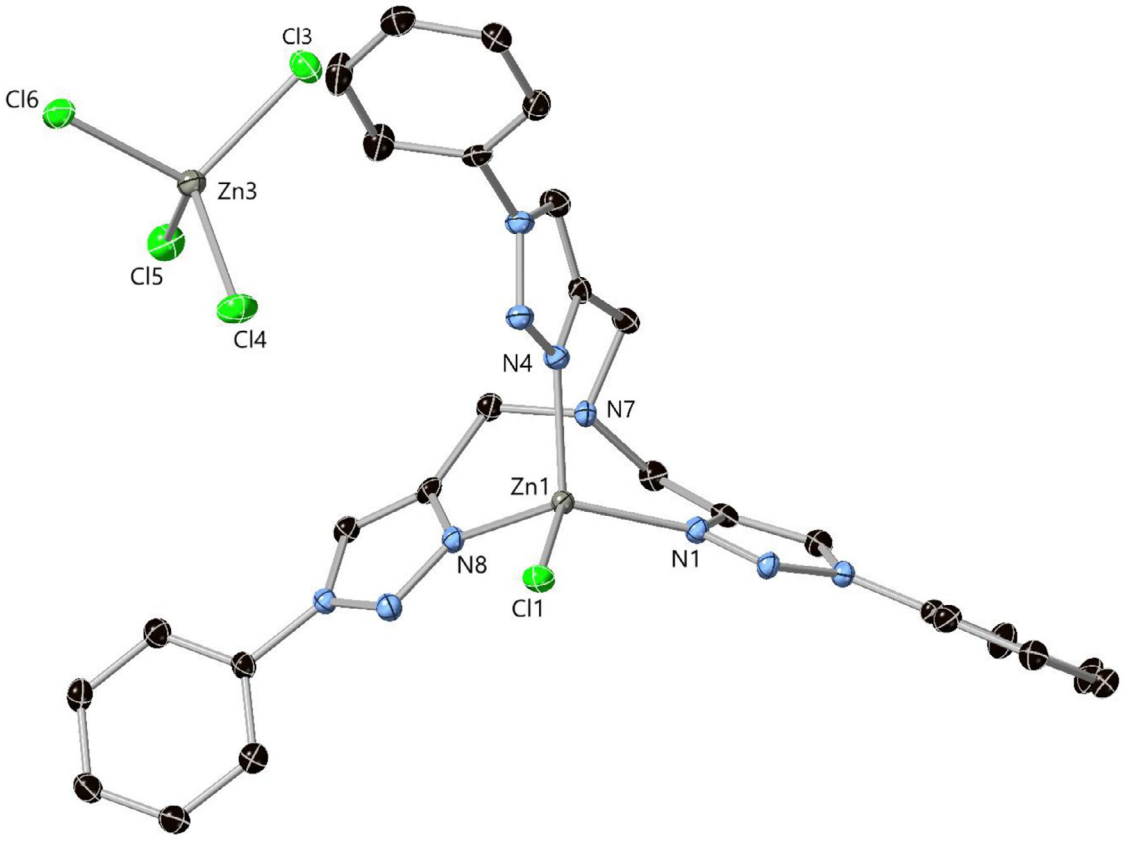

Fig. 8. Structure of complex 4 with partial atom labelling scheme. For clarity only one of the two cationic species is shown, and hydrogen atoms and lattice methanol molecule are omitted. ADPs are rendered at 50% probability level.

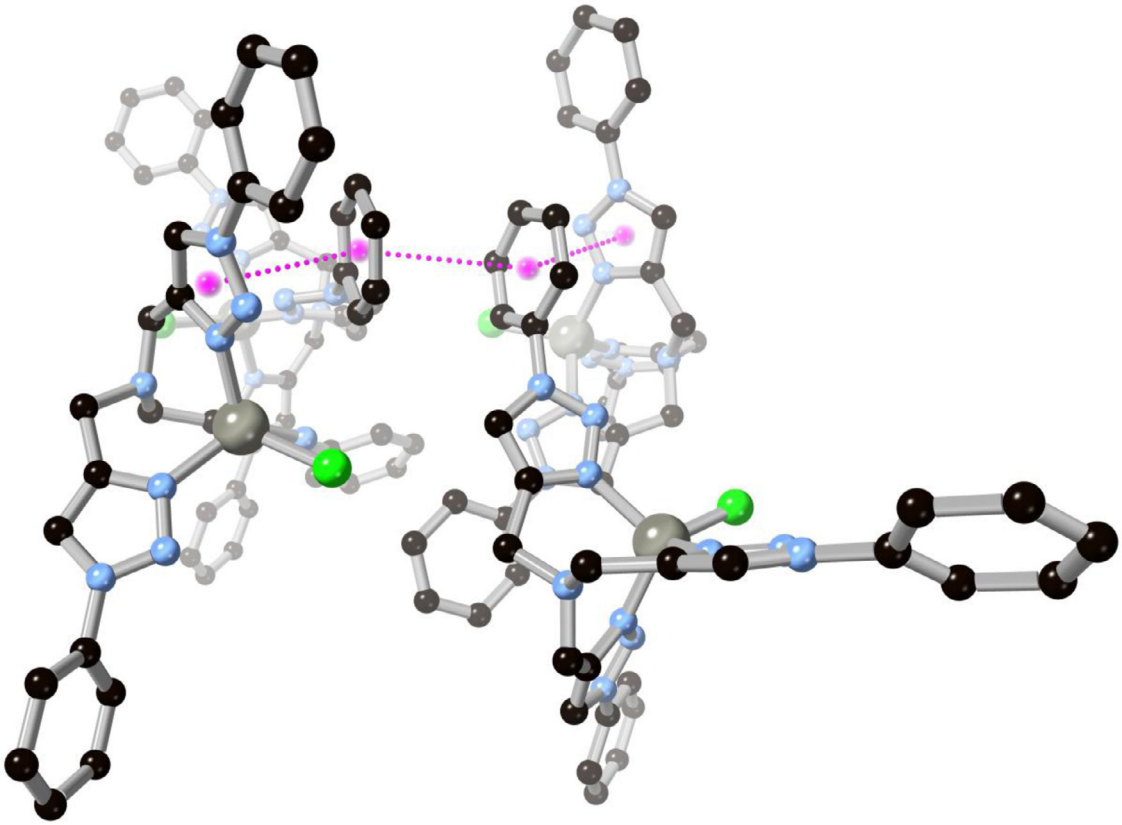

Fig. 9. The $\pi\cdots\pi$ interactions between four cations in the structure of 4. Hydrogen atoms, tetrachlorozincate anions and lattice solvent molecules are omitted for clarity.

tical to those of the free ligand in the same solvent (ESI), suggesting that any association is weak and dynamic in highly competitive media.

4. Conclusions

Here we have reported the synthesis and structural characterisation of four new *d*-block metal complexes of the popular chelating triazole ligands TBTA and TPTA. Despite the chemical similarities of the binding pockets in both species and the similar coordination requirements of the metal ions chosen a range of coordination geometries were observed, from the six-coordinate trigonal prismatic geometry for the manganese complex 1 to the regular octahedral geometry for nickel complex 2, square pyramidal geometry for copper complex 3 and weakly capped tetrahedral zinc complex 4. While all four complexes exhibited the familiar tendencies for intermolecular interactions through $\pi\cdots\pi$ contacts and the triazole C–H hydrogen bond donor, these common influences were largely overruled by classical hydrogen bonding in the case of the hydrated complex 2 or substantial differences in the ligand geometry between the other complexes. Fully understanding and controlling these underlying structural differences is a key step in the rational design of multidentate ligands for base metals with potential for applications in catalysis or molecular magnetism. Solution studies (UV–visible spectroscopy, mass spectrometry and NMR spectroscopy, where appropriate) were used to probe the persistence of complexes 2–4 in solution. These were generally consistent with the findings of the crystallographic study, although complex 1 could not be observed by mass spectrometry suggesting poor solution-phase stability for this complex, and complex 4 (although observed by mass spectrometry) could not be detected by NMR spectroscopy in more competitive media.

Credit author statement

MC undertook all synthetic experimental work, MM collected single crystal X-ray crystallographic data, CSH solved single crystal X-ray data and co-wrote the paper, MW conceived and supervised the research and co-wrote the paper.

Declaration of Competing Interest

There are no conflicts to declare.

Acknowledgements

We are grateful to the EPSRC for the provision of a PhD studentship (to M.C.) and to the EPSRC National Mass Spectrometry Service, University of Wales, Swansea.

Supplementary materials

Supplementary material associated with this article can be found, in the online version, at doi:10.1016/j.molstruc.2022.132736.

References

[1] (a) N.P. Juraj, S.I. Kirin, Inorganic stereochemistry: Geometric isomerism in bis-tridentate ligand complexes, Coord. Chem. Rev. 445 (2021) 214051, doi:10.1016/j.ccr.2021.214051; (b) A.G. Blackman, The coordination chemistry of tripodal tetraamine ligands, Polyhedron 24 (2005) 1–39, doi:10.1016/j.poly.2004.10.012.

[2] (a) G.J.P. Britovsek, J. England, A.J.P. White, Non-heme iron(II) complexes containing tripodal tetradentate nitrogen ligands and their application in alkane oxidation catalysis, Inorg. Chem. 44 (2005) 8125–8134, doi:10.1021/ic0509229; (b) S. Bellemin-Laponnaz, L.H. Gade, A modular approach to C1 and C3 chiral N-tripodal ligands for asymmetric catalysis, Angew. Chem. Int. Ed., Engl. 41 (2002) 3473–3475, doi:10.1002/1521-3773(20020916)41:18⟨3473::AID-ANIE3473⟩3.0.CO;2-N; (c) M.R. Malachowski, H.B. Huynh, L.J. Tomlinson, R.S. Kelly, J.W. Furbee, Comparative study of the catalytic oxidation of catechols by copper(II) complexes of tripodal ligands, J. Chem. Soc., Dalton Trans. (1995) 31–36, doi:10.1039/DT9950000031.

[3] (a) J. Hillenbrand, M. Leutzsch, E. Tiannakas, C.P. Gordon, C. Wille, N. Nöthling, C. Copéret, A. Fürstner, Canopy Catalysts" for alkyne metathesis: Molybdenum alkylidyne complexes with a tripodal ligand framework, J. Am. Chem. Soc. 142 (2020) 11279–11294, doi:10.1021/jacs.0c04742; (b) K. Liu, J.-P. Yu, Q.-Y. Wu, X.-B. Tao, X.-H. Kong, L. Mei, K.-Q. Hu, L.-Y. Yuan, Z.-F. Chai, W.-Q. Shi, Rational design of a tripodal ligand for U(IV): Synthesis and characterization of a U-Cl species and insights into its reactivity, Organometallics 39 (2020) 4069–4077, doi:10.1021/acs.organomet.0c00638; (c) J.-F. Carpentier, Rare-Earth Complexes Supported by Tripodal Tetradentate Bis(phenolate) Ligands: A Privileged Class of Catalysts for Ring-Opening Polymerization of Cyclic Esters, Organometallics 34 (2015) 4175–4189, doi:10.1021/acs.organomet.5b00540.

[4] (a) L.J. Batchelor, E. Fitzgerald, J. Wolowska, J.J.W. McDouall, E.J.L. McInnes, Tripodal thiols as ligands for molecular magnets: very strong antiferromagnetic exchange interactions in vanadium(III) clusters, Chem. Eur. J. 16 (2010) 11082–11088, doi:10.1002/chem.201000823; (b) K.S. Lim, J.J. Baldovi, S. Jiang, B.H. Koo, D.W. Kang, W.R. Lee, E.K. Koh, A. Gaita-Ariño, E. Coronado, M. Slota, L. Bogani, C.S. Hong, Custom coordination environments for lanthanoids: tripodal ligands achieve near-perfect octahedral coordination for two dysprosium-based molecular nanomagnets, Inorg. Chem. 56 (2017) 4911–4917, doi:10.1021/acs.inorgchem.6b03118; (c) H.-R. Wen, P.-P. Dong, S.-J. Liu, J.-S. Liao, F.-Y. Liang, C.-M. Liu, 3d-4f heterometallic trinuclear complexes derived from amine-phenol tripodal ligands exhibiting magnetic and luminescent properties, Dalton Trans 46 (2017) 1153–1162, doi:10.1039/C6DT04027F.

[5] (a) P.A. Scattergood, A. Sinopoli, P.I.P. Elliot, Photophysics and photochemistry of 1,2,3-triazole-based complexes, Coord. Chem. Rev. 351 (2017) 136–154, doi:10.1016/j.ccr.2017.06.017; (b) J. Klein, U. Albold, L. Suntrup, B. Sarkar, How inert are osmium-ligand bonds? A combined thermal, photochemical and electrochemical case study with a click tripodal ligand, ChemPhotoChem 2 (2018) 357–361, doi:10.1002/cptc.201800008; (c) F. Weisser, S. Hohloch, S. Plebst, D. Schweinfurth, B. Sarkar, Ruthenium complexes of tripodal ligands with pyridine and triazole arms: subtle tuning of thermal, electrochemical and photochemical reactivity, Chem. Eur. J. 13 (2014) 781–793, doi:10.1002/chem.201303640.

[6] (a) I. Terao, S. Horii, J. Nakazawa, M. Okamura, S. Hikichi, Efficient alkane hydroxylation catalysis of nickel(II) complexes with oxazoline donor containing tripodal tetradentate ligands, Dalton Trans 49 (2020) 6108–6118, doi:10.1039/D0DT00733A; (b) J. Téllez, I. Méndez, F. Viguri, R. Rodríguez, F.J. Lahoz, P. García-Orduña, D. Carmona, En Route to Chiral-at-Metal Ruthenium Complexes Containing Tripodal Tetradentate Ligands, Organometallics 37 (2018) 3450–3464, doi:10.1021/acs.organomet.8b00180.

[7] (a) Q.V.C. van Hilst, N.R. Lagesse, D. Preston, J.D. Crowley, Functional metal complexes from CuAAC "click" bidentate and tridentate pyridyl-1,2,3-triazole ligands, Dalton Trans. 47 (2018) 997–1002, doi:10.1039/C7DT04570K; (b) E.M. Schuster, M. Botoshansky, M. Gandelman, Pincer click ligands, Angew. Chem. Int. Ed. 47 (2008) 4555–4558, doi:10.1002/anie.200800123; (c) A.F. Henwood, I.N. Hegarty, E.P. McCarney, J.I. Lovitt, S. Donohoe, T. Gunnlaugsson, Recent advances in the development of the btp motif: A versatile terdentate coordination ligand for applications in supramolecular self-assembly, cation and anion recognition chemistries, Coord. Chem. Rev. 449 (2021) 214206, doi:10.1016/j.ccr.2021.214206.

[8] D. Schweinfurth, F. Weisser, D. Bubrin, L. Bogani, B. Sarkar, Cobalt complexes with "click"-derived functional tripodal ligands: Spin Crossover and Coordination Ambivalence, Inorg. Chem. 50 (2011) 6114–6121, doi:10.1021/ic200246v.

[9] T.R. Chan, R. Hilgraf, K.B. Sharpless, V.V. Fokin, Polytriazoles as copper(I) stabilizing ligands in catalysis, Org. Lett. 6 (2004) 2853–2855, doi:10.1021/ol0493094.

[10] Q. Wang, T.R. Chan, R. Hilgraf, V.V. Fokin, K.B. Sharpless, M.G. Finn, Bioconjugation by Copper(I)-Catalyzed Azide-Alkyne [3 + 2] Cycloaddition, J. Am. Chem. Soc. 125 (2003) 3192–3193, doi:10.1021/ja021381e.

[11] (a) D. Schweinfurth, S. Demeshko, S. Hohloch, M. Steinmetz, J.F. Brandenburg, S. Dechert, F. Meyer, S. Grimme, B. Sarkar, Spin Crossover in Fe(II) and Co(II) complexes with the same click-derived tripodal ligand, Inorg. Chem. 53 (2014) 8203–8212, doi:10.1021/ic500264k; (b) D. Schweinfurth, J. Krzystek, I. Schapiro, S. Demeshko, J. Klein, J. Telser, A. Ozarowski, C.-Y. Su, F. Meyer, M. Atanasov, F. Neese, B. Sarkar, Electronic Structures of Octahedral Ni(II) Complexes with "Click" Derived Triazole Ligands: A Combined Structural, Magnetometric, Spectroscopic, and Theoretical Study, Inorg. Chem. 52 (2013) 6880–6892, doi:10.1021/ic3026123; (c) D. Schweinfurth, J. Klein, S. Hohloch, S. Dechert, S. Demeshko, F. Meyer, B. Sarkar, Influencing the coordination mode of tbta (tbta = tris[(1-benzyl-1H-1,2,3-triazol-4-yl)methyl]amine) in dicobalt complexes through changes in metal oxidation states, Dalton Trans 42 (2013) 6944–6952, doi:10.1039/C3DT00102D.

[12] P.S. Donnelly, S.D. Zanatta, S.C. Zammit, J.M. White, S.J. Williams, Click' cycloaddition catalysts: copper(I) and copper(II) tris(triazolylmethyl)amine complexes, Chem. Commun. (2008) 2459–2461, doi:10.1039/B719724A.

[13] M.G. Sommer, R. Marx, D. Schweinfurth, Y. Rechkemmer, P. Neugebauer, M. van der Meer, S. Hohloch, S. Demeshko, F. Meyer, J. van Stageren, B. Sarkar, Control of complex formation through peripheral substituents in click-tripodal ligands: structural diversity in homo- and heterodinuclear cobalt-azido complexes, Inorg. Chem. 56 (2017) 402–413, doi:10.1021/acs.inorgchem.6b02330.

[14] M. Ostermeier, M.-A. Berlin, R.M. Meudtner, S. Demeshko, F. Meyer, C. Limberg, S. Hecht, Complexes of Click-Derived Bistriazolylpyridines: Remarkable Electronic Influence of Remote Substituents on Thermodynamic Stability as well as Electronic and Magnetic Properties, Chem. Eur. J. 16 (2010) 10202–10213, doi:10.1002/chem.201000721.

[15] (a) A. Baschieri, A. Mazzanti, S. Stagni, L. Sambri, Triple Click to Tripodal Triazole-Based Ligands – Synthesis and Characterization of Blue-Emitting Ce3+ Complexes, Eur. J. Inorg. Chem. 13 (2013) 2432–2439, doi:10.1002/ejic.201201361; (b) J.E. Hein, L.B. Krasnova, M. Iwasaki, V.V. Fokin, Cu-CATALYZED AZIDE-ALKYNE CYCLOADDITION: PREPARATION OF TRIS((1-BENZYL-1H-1,2,3-TRIAZOLYL)METHYL)AMINE, Org. Synth. 88 (2011) 238–246, doi:10.15227/orgsyn.088.0238.
[16] K. De Buysser, G.G. Herman, E. Bruneel, S. Hoste, I. Van Driessche, Determination of the number of unpaired electrons in metal-complexes. A comparison between the Evans' method and susceptometer results, Chem. Phys. 315 (2005) 286–292, doi:10.1016/j.chemphys.2005.04.022.
[17] Bruker APEX-3, Bruker-AXS Inc., Madison, WI, 2016.
[18] SADABS, Bruker-AXS, Madison, WI, 2016.
[19] G.M. Sheldrick, SHELXT – Integrated space-group and crystal-structure determination, Acta Crystallogr. Sect. A.: Found. Adv. 71 (2015) 3–8, doi:10.1107/S2053273314026370.
[20] G.M. Sheldrick, Crystal structure refinement with SHELXL, Acta Crystallogr. Sect. C.: Struct. Chem. 71 (2015) 3–8, doi:10.1107/S2053229614024218.
[21] O.V. Dolomanov, L.J. Bourhis, R.J. Gildea, J.A.K. Howard, H. Puschmann, OLEX2: a complete structure solution, refinement and analysis program, J. Appl. Cryst. 42 (2009) 339–341, doi:10.1107/S0021889808042726.
[22] H. Hadadzadeh, G. Mansouri, A. Rezvani, H.R. Khavasi, B.W. Skelton, M. Makha, F.R. Charati, Mononuclear nickel(II) complexes coordinated by polypyridyl ligands, Polyhedron 30 (2011) 2535–2543, doi:10.1016/j.poly.2011.06.037.
[23] A.W. Addison, T.N. Rao, J. Reedijk, J. van Rijn, G.C. Verschoor, Synthesis, structure, and spectroscopic properties of copper(II) compounds containing nitrogen-sulphur donor ligands; the crystal and molecular structure of aqua[1,2-bis(*N*-methylbenzimidazol-2'-yl)-2,6-dithiaheptane]copper(II) perchlorate, J. Chem. Soc., Dalton Trans. (1984) 1349–1356, doi:10.1039/DT9840001349.
[24] M.A. Spackman, D. Jayatilaka, Hirshfeld surface analysis, CrystEngComm 11 (2009) 19–32, doi:10.1039/B818330A.
[25] K.D. Karlin, J.C. Hayes, S. Huen, J.P. Hutchinson, J. Zubieta, Tetragonal vs. trigonal coordination in copper(II) complexes with tripod ligands: structures and properties of [Cu(C21H24N4)Cl]PF6 and [Cu(C18H18N4)Cl]PF6, Inorg. Chem. 21 (1982) 4106–4108, doi:10.1021/ic00141a049.